**Proceedings of ASME Turbo Expo 2017: Turbine Technical Conference and Exposition**
**GT2017**
**June 26-30, 2017, Charlotte, NC, USA**

# GT2017-64021

# INVESTIGATION OF TIP CLEARANCE FLOW EFFECTS ON AN OPEN 3D STEAM TURBINE FLUTTER TEST CASE

**Tianrui Sun**
Department of Energy Technology
Royal Institute of Technology
Stockholm, Sweden
tianrui@kth.se

**Paul Petrie-Repar**
Department of Energy Technology
Royal Institute of Technology
Stockholm, Sweden
paul.petrie-repar@energy.kth.se

**Di Qi**
Department of Energy Technology
Royal Institute of Technology
Stockholm, Sweden
diq@kth.se

## ABSTRACT

Blade failure caused by flutter is a major problem in the last stage of modern steam turbines. It is because rotor at this stage always has a large scale in spanwise, which provides low structural frequency as well as supersonic tip speeds. Since most of the unsteady aerodynamic work is done in the tip region, transonic tip-leakage flow that influences the tip region flow could have a remarkable effect on the aerodynamic stability of rotor blades. However, few research had been done on the tip-leakage flow influence on flutter characteristic based on full-scale steam turbine numerical models. In this paper, an open 3D steam turbine stage model designed by Durham University was applied, which was widely analyzed and representative for the last stage of modern industrial steam turbines. The average Mach number at the rotor outlet is 1.1. URANS simulation carried by both numerical software CFX and LUFT code is applied, and the two solvers show an agreement on steady and unsteady results. The numerical results indicate that the influence of tip leakage flow on blade stability is based on two types of flow mechanisms. Both mechanisms act on the suction side of near tip region. The first type of mechanism is produced by the reduction of passage shock near the leading edge, and the other type of mechanism at the rear of blade is caused by the interaction between tip leakage vortex and trailing edge shock of the neighbor blade. In conclusion, tip leakage flow has a significant influence on steam turbine flutter boundary prediction and requires further analysis in the future.

**Keywords**: Steam turbine, aerodynamic stability, flutter, tip clearance

## NOMENCLATURE

| | |
|---|---|
| $\alpha$ | the ratio of maximum blade displacement to chord at mid-span |
| $\Xi$ | non-dimensional aerodynamic damping |
| $w^*$ | reduced frequency |
| $b$ | blade height |
| $c$ | chord at mid-span |
| $f$ | modal frequency |
| $\boldsymbol{h}$ | amplitude of local displacement |
| $h_{max}$ | maximum blade displacement |
| $\bar{n}$ | local normal vector |
| $p_i$ | imaginary component of the local unsteady pressure |
| $p_{ref}$ | reference pressure |
| $w$ | local work coefficient |
| $V_{ref}$ | relative velocity at turbine exit |
| $W_{aero}$ | average unsteady work per cycle |

## 1 INTRODUCTION

The last stage of modern steam turbines tends to be longer and thinner nowadays to meet the need of high efficiency. However, the long span and low natural frequency of blades impair the aeroelastic stability. As a self-excited vibration generated by fluid-structure interaction, flutter can induce blade failure in a short period of time. Since most of the unsteady

aerodynamic work is done in the tip region, the tip leakage flow could have remarkable effects on blade aerodynamic stability. The tip leakage flow driven by pressure gradient starts from the pressure side of the blade and moving to suction side in tip clearance, and a tip leakage vortex will be formed under the interaction between tip leakage flow and the main flow [1-2].

Sanders [3] found that the transonic tip clearance flow could had an impact on the unsteady loading on the suction side of the low aspect ratio fan blisk, though the clearance flow has little effect on the time-average flow field. He suggested considering tip clearance flow could enhance the accuracy of flutter boundary prediction in comparison with experimental results. Variation of tip clearances could also influence the stability of compressor blade [4-7]. Besem [5] illustrated that the aerodynamic damping of the blade first increases with the gap size and then rapidly decreases. Meanwhile, the study carried by Fu [7] indicated that the aerodynamic stability of compressor would be reduced first with tip gap increasing until a most-dangerous tip gap size and then increased.

Similar studies[8-10] have been performed for turbines. Glodic[9] performed experiments in the KTH AETR (Aeroelastic Turbine Rig) with an oscillating turbine blade in a partial annulus with an exit Mach number of 0.4. 3D URANS simulations of the experimental setup showed that a better agreement with the experiment results were achieved if the tip clearance was included in the computational model. It was found that the model without the tip gap gave over-conservative damping predictions compared with experimental results. However, the overall influence of the tip gap flow on the aerodynamic damping was small. Teixeira[8] extended the computations of the KTH AETR to higher exit Mach numbers (0.74) and the conclusions were similar to those found by Glodic. Experimental and numerical results performed by Huang [10] on a low-speed linear turbine cascade shown that tip clearance could show stability effects at 1.25% and 2.5% chord, for the tip leakage flow provides a stability contribution around the mid-chord on the suction surface near the tip. With a large tip clearance such as 5% chord, the stability contribution would be offset by the fully-developed tip leakage flow around 80% chord. Comparison between experimental and CFD results in this analysis showed that the tip leakage flow influence on turbine blade flutter could be successfully captured by numerical simulation. The isentropic exit Mach number applied in Huang's numerical simulation is 0.3.

While the previous work on the influence of tip clearance flow on flutter stability for turbines did show a detectable difference on aerodynamic damping, the change in the overall damping curves were small. However, most of the previous studies were for low speeds and low stagger angles. The highest Mach number examined in the previous work was 0.74. It is speculated that the influence of the tip clearance flow on flutter will be greater for higher Mach number flows and for turbines with higher stagger angles because of the higher pressure difference across the blade. In this paper a recently developed flutter test case for a 3D steam turbine blade will be examined. Here the exit Mach number is 1.1 and the stagger angle near the tip is 67 degrees. The aim of this study is to investigate the influence of the tip clearance flow for the 3D steam turbine flutter test case and the physics behind the differences observed. The phenomena were investigated by performing unsteady flow simulations using two independently developed URANS flow solvers which have been extensively validated. The URANS model is the highest fidelity model that is currently used for flutter analysis. It has been shown in studies on transonic compressors[11-13], that the URANS model can capture the main tip leakage flow structure at transonic and high stagger angle tip region.

The influence of tip clearance on steady flow was investigated first, then the comparison of aerodynamic damping for cases with and without tip clearance showed the significant influence of tip leakage flow on blade aerodynamic damping. Plots of aerodynamic work on the blade as a function of span and work coefficient near the tip were shown to highlight the influence of tip clearance flow on flutter. At the end of this study, the influence of tip leakage flow on blade stability is classified as two difference flow mechanisms, which will be illustrated in detail in the discussion part.

## 2 METHODOLOGY

In this study, the energy method is used to perform the flutter analysis. It is assumed that the aeroelastic modes are travelling wave modes and 3D URANS flow simulations are performed to calculate the unsteady aerodynamic work on the blade due to a prescribed blade motion at various interblade phase angles. The natural modal of blade vibration is obtained by ANSYS APDL, and two CFD solvers including ANSYS CFX and LUFT are applied. The LUFT code is a linearized unsteady fluid solver which has been validated for turbomachinery flutter analysis [14,15].

Numerical simulation of steady state includes both stator and rotor blades of the steam turbine stage. In the simulation carried by CFX, the k- $\epsilon$ turbulence model with automatic wall functions is applied for fluid field simulation, and the turbulence model used by LUFT is Spalart and Allmaras model which has been fully linearized for the unsteady flow analysis. The turbulence intensity at the inlet boundary is set to 10%. The time-transformation method is applied on different traveling wave modes in CFX unsteady simulation. The total pressure and the velocity at the stator/rotor interface extracted from the steady results is applied as the inlet boundary condition of unsteady simulation. Only the rotor domain is considered in the unsteady calculation. Standard periodic boundary conditions were applied at the periodic boundaries, and the passage number is determined by the inter-blade phase angle. For example, four passages were used when IBPA equals ±90º, and two passages were used for IBPA equals 180º. Sixty-five time steps are included in a blade vibration period, with maximum 20 inner iterations per time step. The maximum amplitude of the blade vibration was set to 2.05 mm for the unsteady CFX calculations.

For the unsteady results, non-dimensional aerodynamic damping is defined as follows:

$$\Xi = \frac{-W_{aero}}{\pi b \alpha^2 c^2 p_{ref}} \quad (1)$$

where $\Xi$ is the non-dimensional aerodynamic damping, $W_{aero}$ is the unsteady work, $b$ is the blade height, $p_{ref}$ is the reference pressure, $\alpha$ equals $h_{max}/c$, in which $h_{max}$ is the maximum blade displacement and $c$ is the middle chord length. The reference pressure is equal to the average total pressure minus the average static pressure at the inlet of the rotor.

To capture the local aerodynamic stability on the blade surface, local work coefficient is applied:

$$w = \frac{-\boldsymbol{h}\cdot\bar{n}p_i}{\alpha^2 c p_{ref}} \quad (2)$$

where $w$ is the local work coefficient, $\boldsymbol{h}$ is the local displacement factor, $\bar{n}$ is the local normal vector and $p_i$ is the imaginary component of the local unsteady pressure.

The unsteady CFX simulation were run until a time periodic flow solution was achieved.

## 3 GEOMETRIC MODEL

The Open-3D test case used in this study is a realistic-scale last stage steam turbine stage with both stator and rotor. The geometry and boundary conditions are available online [16]. The test case was firstly applied by Durham University in the simulation of exhaust hood flows. Schematic figure of this stage is shown in Fig.1. The rotor rotates at 3000 rpm with a maximum 920 mm length of blades. The average inlet flow conditions are total pressure 27 kPa and total temperature 340 K, and the average isentropic exit Mach number equals 1.12, which are typical for the last stage of steam turbines. The average static pressure at the exit of the diffuser is 8800 Pa. Similar to industrial steam turbines, transonic flow is shown in the tip region and near the tip of rotor blades a 67 degrees high stagger angle is presented. The stage has representative geometrical parameters and flow boundary conditions of modern last stage steam turbine.

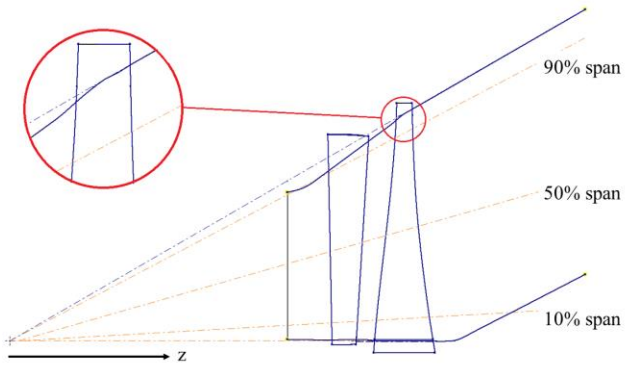


**Figure 1 Schematic figure of test steam turbine and span lines**

Two rotor models based on this geometry are studied, one is set as no tip clearance and the other has a uniform tip clearance value equals 0.25% span length (2.3 mm), which is typical in the industry steam turbines. The resolution of the mesh in the tip clearance region was 30 cells in the span direction. The tip surface was parallel to the shroud surface. The computational meshes for fluid domain of both models are generated by TurboGrid. TurboGrid uses a non 1:1 mesh interface to connect the meshes from the pressure and suction side in the tip clearance. The average y-plus of the cell height on the walls equals 40 in the mesh applied in CFX simulation, and in LUFT calculation the average y-plus for the first-layer mesh is 1.2. Based on mesh independence analysis, the LUFT mesh has 0.95 million cells, the CFX mesh without tip clearance has 0.83 million cells, and the CFX mesh with tip clearance has 1.02 million cells. Minimum face angles of the three meshes are larger than 38 degrees. Figure 2 shows the rotor domain and the blade to blade mesh at the middle span applied in this study.

The whole diffusor is included in the rotor domain in the CFX calculation to reduce the influence of boundary reflection from the outlet. In the simulation carried by LUFT, since the non-reflecting boundary condition is applied, the diffusor outside of the mixing plane is not included in the unsteady calculations. The independence of unsteady results from outlet boundary position in LUFT code had been verified in Ref. 17.

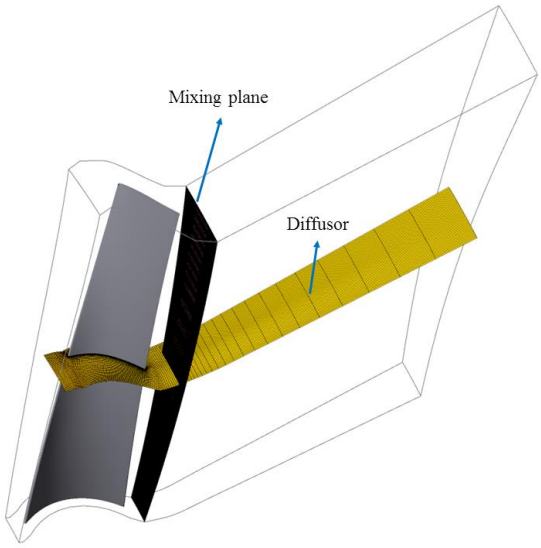


**Figure 2 Rotor domain and blade to blade mesh at the middle span**

The first bending modal of the rotor blade is applied in the unsteady simulation in this study. The blade shape at hot condition is applied in the modal calculation in this paper. The fixed root assumption is used to obtain the mode shape as an approximation for blade dominated mode shapes. Pre-stress and spin softening are both considered in the modal calculation. The mode shape of the first bending modal is shown in Fig.3. The natural frequency of this modal shape calculated by ANSYS is 92.878 Hz, which correspond to a reduced frequency $w^*$ equals almost 0.2 from the following equation:

$$w^* = \frac{wc}{V_{ref}} = \frac{2\pi f c}{V_{ref}} \quad (3)$$

in which $f$ is modal frequency, $c$ is chord length, $V_{ref}$ is average relative velocity at turbine exit. The open geometry from Durham was design based on only aerodynamic

considerations but not structural dynamics. As a result, the frequency of the first mode is lower than the expect for a real steam turbine application. In this study, the vibration frequency applied in unsteady simulations was modified to a reduced frequency equals 0.3. The modified modal frequency is calculated by Eq. 3 and equals 132.08Hz.

**Figure 3: The first bending mode**

In order to build an open model that could be compared by other researchers, a straight definition of span surface is necessary. In this study, two lines that approximate to rotor hub/shroud curve projection in Z-R plane are chosen as 0% and 100% span. Specifically, the 0% span line has a constant radius R=0.713m. The 100% span line is represented by a straight line with gradient $k = 0.577$. The line that crosses the intersection point of 0% and 100% span line with a slope of $x\% * k$ is defined as the $x\%$ span line, the cone surface generated by the rotating of the $x\%$ span line along the $Z$ axis is defined as the $x\%$ span surface. The 10% span line, 50% span line, and 90% span line are showed in Fig.1. The equation describes the $x\%$ span line is Eq. 4, in which R is the position in radial coordinate, Z is the position in rotating axis.

$$R = 0.713[m] + k * (Z + 1.102[m]) \quad (4)$$

## 4 RESULTS AND DISCUSSION

### 4.1 Steady state analysis

Steady state simulations with no tip clearance model were performed by both CFX and LUFT, while the steady state of the model with tip clearance is only calculated by CFX. Simulated total performance parameters of the whole stage at steady state are listed in Table 1, in which the total parameters in different solver and different tip clearance model do not vary much.

**Table 1 Total parameters of rotor domain in steady state**

| | LUFT_notip | CFX_notip | CFX_tip |
|---|---|---|---|
| Mass(kg/s) | 86.42 | 85.62 | 85.66 |
| Power (MW) | 11.62 | 11.93 | 11.86 |
| Total to static isentropic efficiency (%) | 84.32 | 84.13 | 84.21 |

The Mach number contour at 50%, 90%, and 98% span of the two cases calculated by CFX are shown in Fig. 4, 5, and 6. The Mach number distribution at 50% span are very similar for both cases, which illustrates that the tip leakage flow does not have a significant influence on the flow at 50% span. Meanwhile, a low-Mach number region near the suction side of the blade from Fig 5 and 6 shows that the tip-leakage flow could have a significant influence on the flow field higher than 90% span.

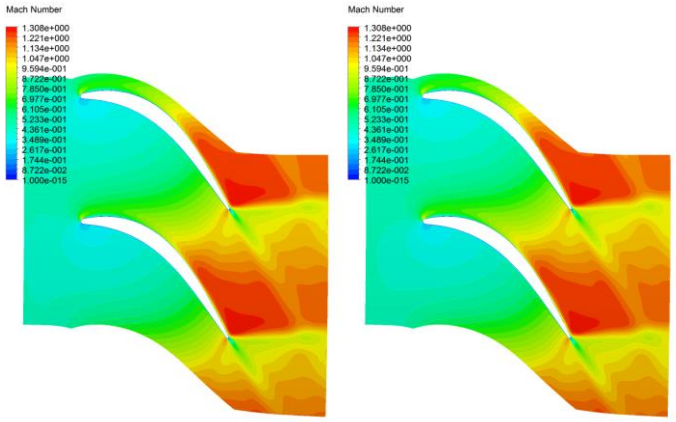


**Figure 4 Mach contour at 50% span, left: no tip clearance model; right: model with tip clearance**

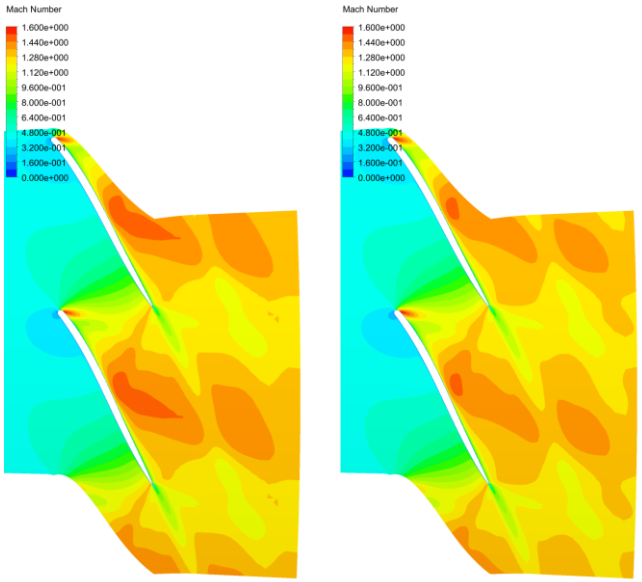


**Figure 5 Mach contour at 90% span, left: no tip clearance model; right: model with tip clearance**

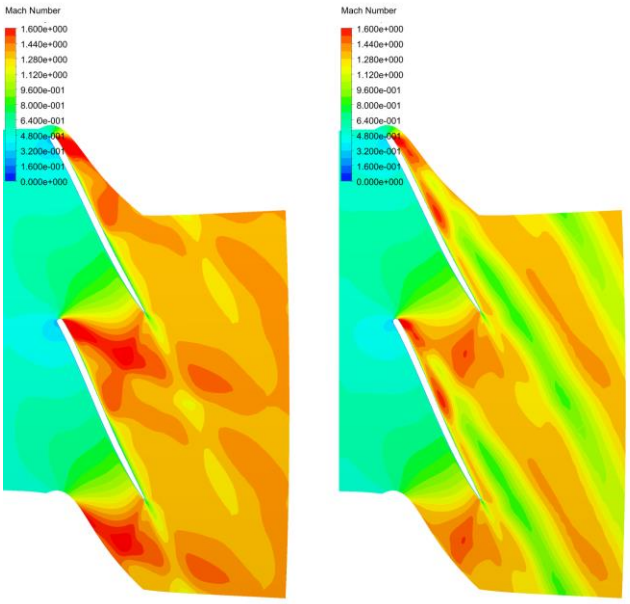


**Figure 6 Mach contour at 98% span, left: no tip clearance model; right: model with tip clearance**

The same conclusion could be made by comparison of the blade loading. Pressure distributions calculated by CFX and LUFT at 50%, 90%, and 98% span are shown in Fig. 7, 8, and 9. The results by both solvers for the no tip clearance model fits well. With the consideration of tip clearance, there is increase in loading on the suction surface in the frontal region and towards the rear at both 50% and 90% span. At the suction side 98% span, the loading increase effect in the frontal region moving towards to the trailing edge with an increased amplitude, meanwhile, there is an unloading region towards the rear in the model with tip clearance. Pressure distribution almost unchanged on the pressure side of the two models calculated by CFX. The variation of pressure distribution indicates that the tip leakage flow influences the flow field, especially on the suction side at near tip region. The streamline and Mach number contour at Z constant planes (Fig. 10) show the structure of tip leakage flow better. The tip leakage vortex generates a low Mach number region on the suction side of the blade, which have an increasing trend of influence area along the chord.

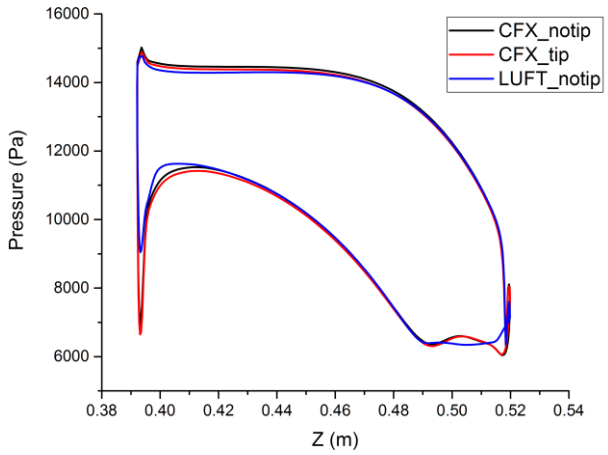


**Figure 7 Blade steady pressure distribution at 50% span**

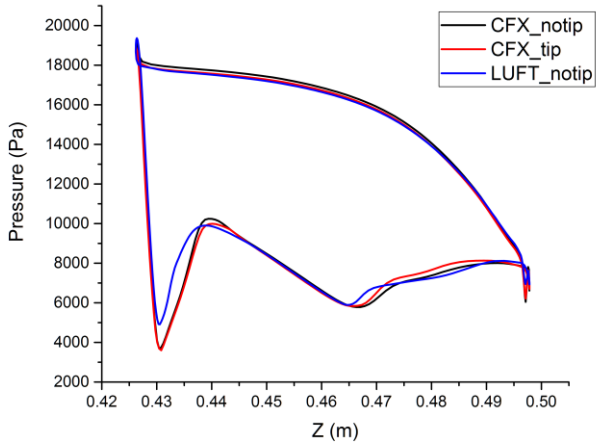


**Figure 8 Blade steady pressure distribution at 90% span**

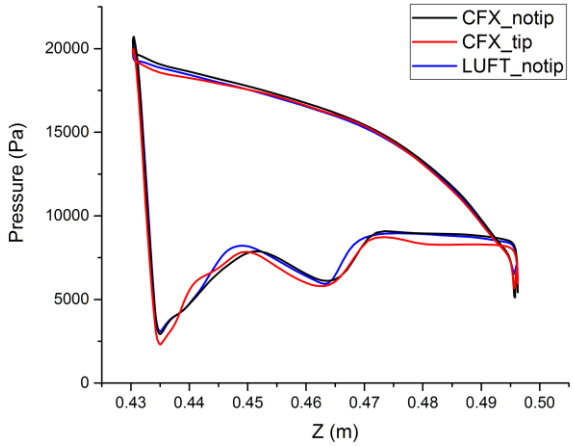


**Figure 9 Blade steady pressure distribution at 98% span**

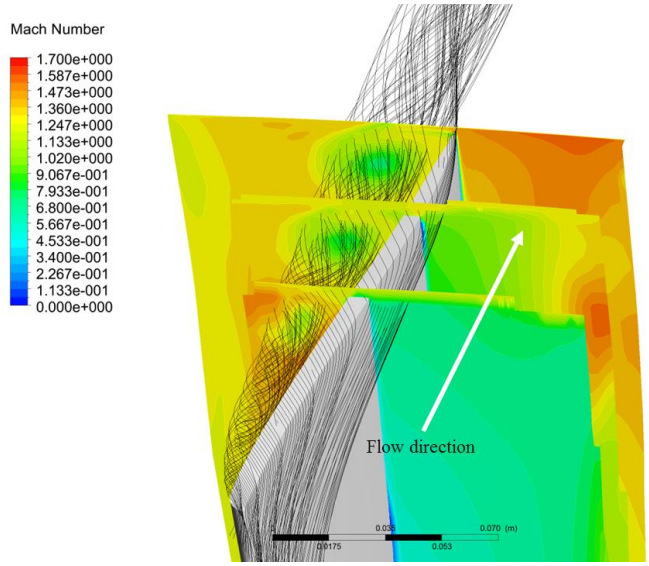


**Figure 10 The structure of tip clearance flow**

The influence of tip clearance flow on shock and wake structure could be shown in the schlieren plots from Fig. 11 to Fig. 13. The flow structure at 50% span is almost unchanged. Meanwhile, the strength of shock at the leading edge is reduced in the tip region of suction side at 90% span, which could be caused by the reduction of flow energy generated by the tip clearance loss. At 98% span, the flow structure is very different in two models because of the interaction between tip clearance flow and the trailing edge wake generated by the neighbor blade.

Since most of the unsteady work done on the blade due to flutter is done near the tip, it is assumed that changes in the time averaged flow near the tip will influence the flutter stability. Analysis on the unsteady characteristic will be presented in the next section, and the specific influence on aerodynamic damping by tip leakage flow would be discussed in section 4.3.

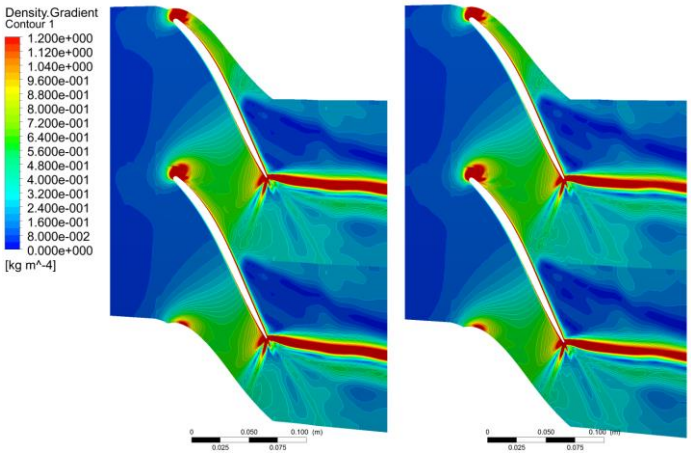


**Figure 11 Schlieren plots at 80% span, left: no tip clearance model; right: model with tip clearance**

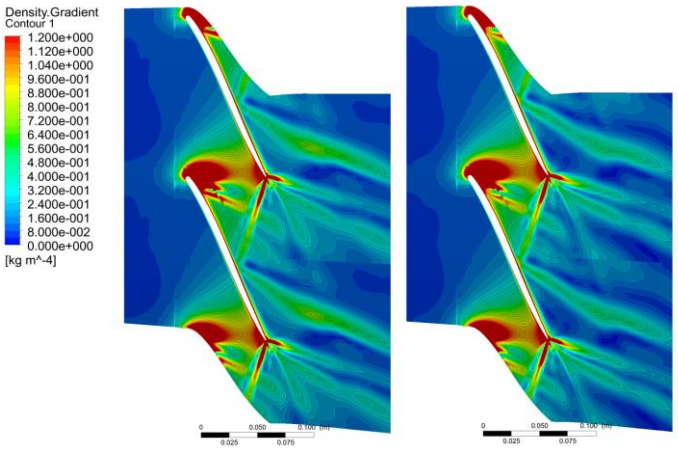


**Figure 12 Schlieren plots at 90% span, left: no tip clearance model; right: model with tip clearance**

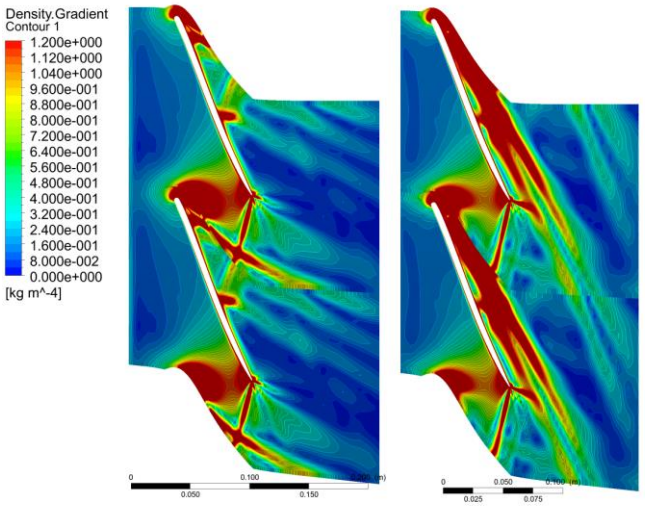


**Figure 13 Schlieren plots at 98% span, left: no tip clearance model; right: model with tip clearance**

## 4.2 Unsteady state analysis

The aerodynamic damping as a function of inter-blade phase angle (IBPA) is shown in Fig. 14. The shape of the curve is a typical for a stage steam turbine. Although the damping value calculated by LUFT and CFX vary, the trend is similar.

At the least stable IBPA calculated by CFX (-45 degree), the model with tip clearance is more stable than that without tip clearance.

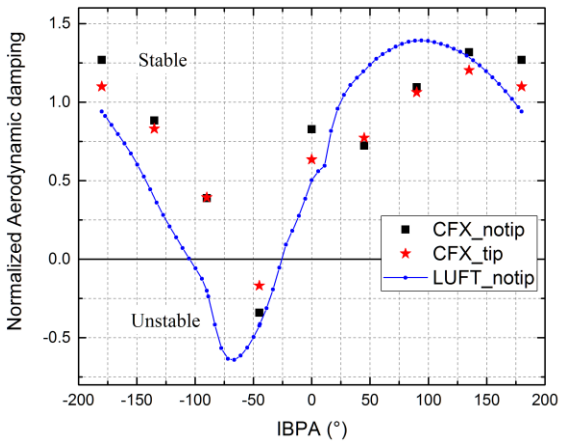


**Figure 14 Aerodynamic damping versus IBPA**

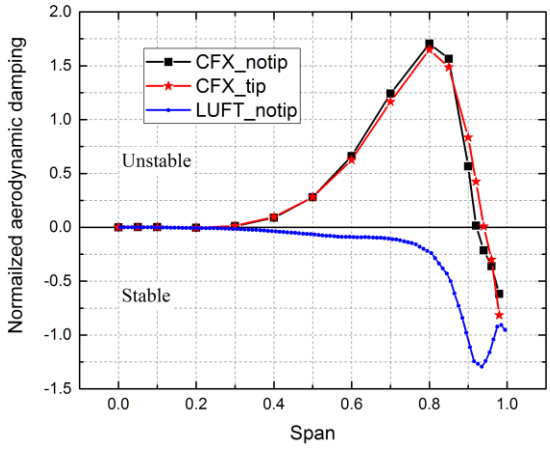


**Figure 15 Aerodynamic damping versus span at -90° IBPA**

In Fig. 14, we can see an aerodynamic damping value difference between CFX results and LUFT results. The maximum difference between the two solvers occurs at -90 degrees. Here, the predicted damping is stable for CFX, but the LUFT calculation results indicates instability.

Comparison of the local work coefficient distribution versus span in Fig. 15 highlights the difference. The local work coefficient at 90% span in Fig. 16 have the similar shape between the two solvers, however, the absolute value at both suction and pressure side shows significant difference. The distribution pattern of local wall work calculated by CFX and LUFT are similar but there are some differences. These differences are probably due to reflections from the out let within the CFX simulation and the fact that LUFT simulations are using a high resolution mesh in the boundary layer. Another possible reason is that LUFT could not capture non-linear effects. Specific reasons for the differences is still unknown and needed to be analyzed in the future. In the following discussion, we will focus on the comparison of the CFX solutions to highlight the influence of the tip clearance flows, and the LUFT results are included as a reference.

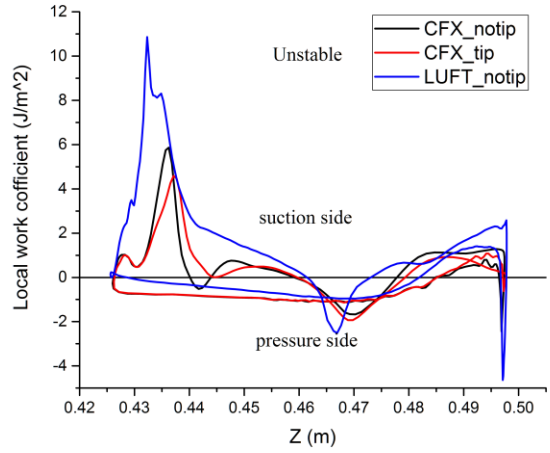


**Figure 16 Local work coefficient at 90% span at -90° IBPA**

To analysis the physical mechanics of the stabilization phenomenon, the aerodynamic damping at each span of the rotor blade at -45 degree IBPA is showed in Fig. 17. The aeroelastic damping values are calculated from local work coefficient at each span and then normalized by the maximum amplitude of the whole blade. It can be seen the most of the aerodynamic work contributing to flutter occurs near the tip. Comparing the CFX results on the two models, a stabilization effect in the whole span is shown with tip clearance, especially at the near tip region.

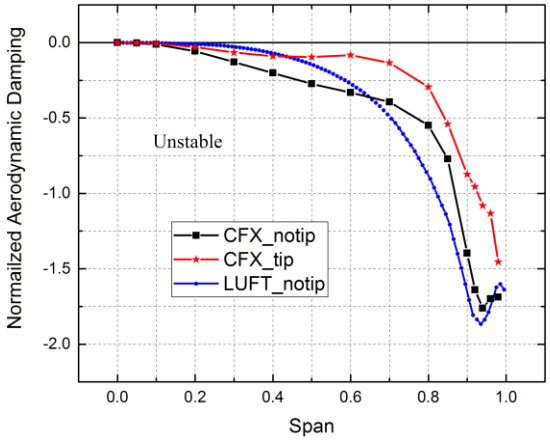


**Figure 17 Aerodynamic damping versus spans at -45° IBPA**

The distribution of local work coefficient (positive represents unstable) at 50%, 90%, and 98% span are shown in Fig. 18, 19, and 20 to further analyze the mechanism of the difference between aerodynamic damping at each span.

In Fig. 18, a stabilization effect could be seen at the pressure side of 50% span. Since most aerodynamic work is in the near tip region, the difference of local aerodynamic at near tip region is focused. At 90% span, two stabilization region could be seen on the suction side, one near the leading edge and the other is nearing the trailing edge. At 98% span, the stability effect near the front region is reduced, meanwhile, the influence region at the rear region is lengthened. The two region contributes to most of the stabilization effect generated by the tip clearance influence.

It is natural to combine the aerodynamic stability variation to the time-averaged flow structure change caused by tip leakage flow. Mechanism of this phenomenon will be discussed in the following section.

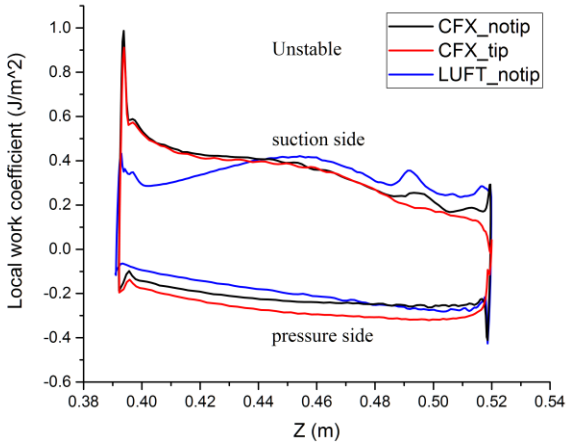


**Figure 18 Local work coefficient at 50% span at -45° IBPA**

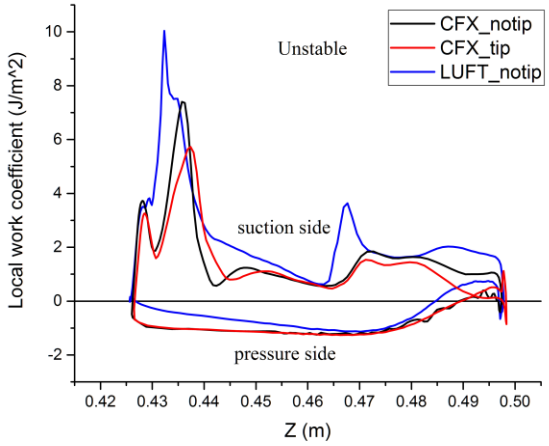


**Figure 19 Local work coefficient at 90% span at -45° IBPA**

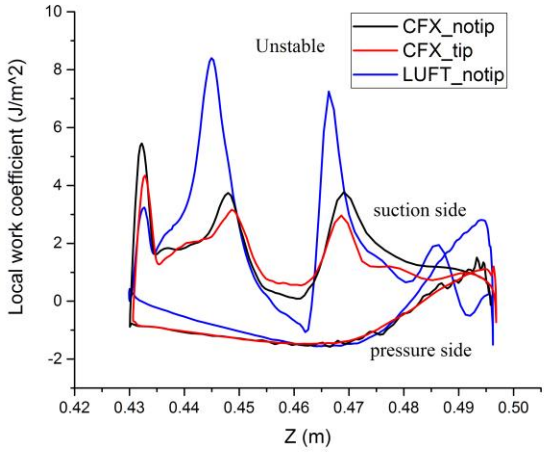


**Figure 20 Local work coefficient at 98% span at -45° IBPA**

## 4.3 Analysis of physical mechanisms

It could be concluded that most influence on blade stability occurs at the near tip region on the suction side. Thus, the local work coefficient contour at -45 ° IBPA (positive represents unstable) is shown in Fig. 21 to Fig. 23 to help us understanding the mechanism. Similar distribution pattern could be seen in CFX and LUFT results.

Comparing Fig. 22 and Fig. 23, two significant stabilization regions can be seen. The first stabilization region is located at the passage shock near the leading edge. The second region is where the trailing edge shock impinges on the suction surface near mid-chord. These flow structures can also be seen in Fig.12 and 13, as well as Fig.24 and 25.

As it discussed in Section 4.1 and 4.2, losses caused by tip clearance flow weaken the strength of passage shock, which reduces the instability at the leading edge of tip region. The other stabilization region is a near-horizontal zone near the tip. In this region, which is generated by the interaction of tip leakage flow and trailing edge shock generated in the neighbor blade reduced

the aerodynamic work on the blade. Influence region by this mechanism expands in spanwise in the flow direction.

Combining with the analysis in section 4.1 and section 4.2, the influence of tip clearance flow on blade flutter characteristics is mainly caused by the two types of mechanisms discussed above. Both of the mechanics are generated by the transonic flow at the tip region of the last stage of steam turbine, which indicates that they could not be captured in low-speed turbine experiments.

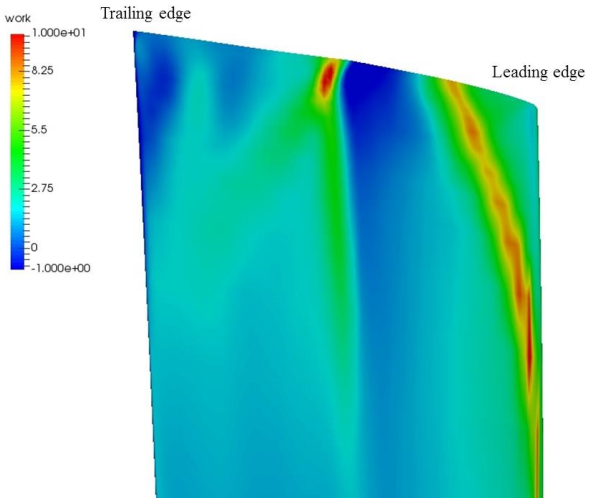


**Figure 21 Local work coefficient at tip region of blade suction side with no tip model calculated by LUFT**

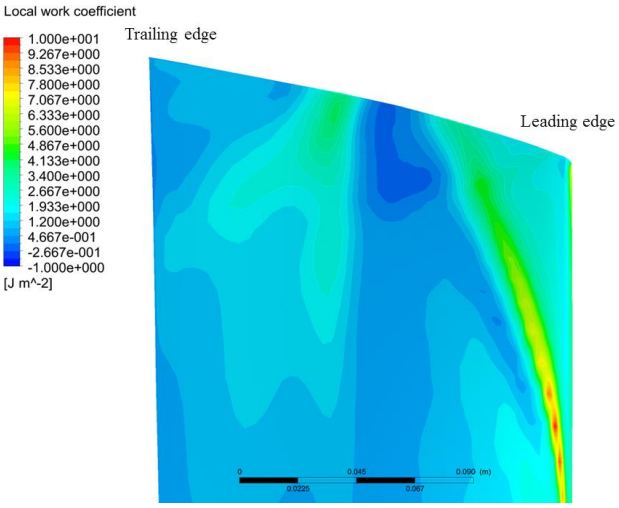


**Figure 22 Local work coefficient at tip region of blade suction side with no tip model calculated by CFX**

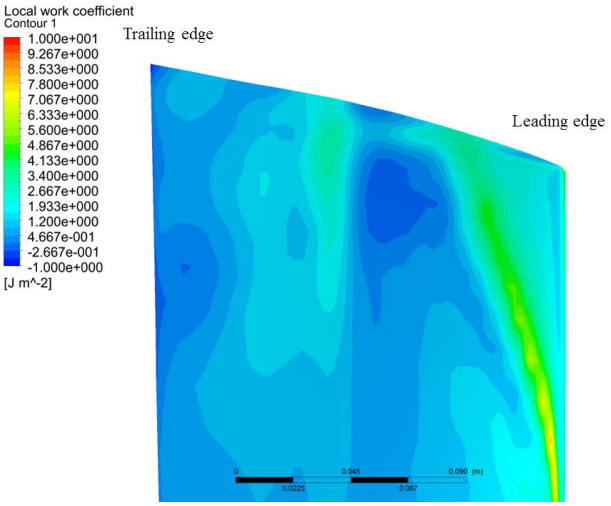


**Figure 23 Local work coefficient at tip region of blade suction side with model with tip clearance calculated by CFX**

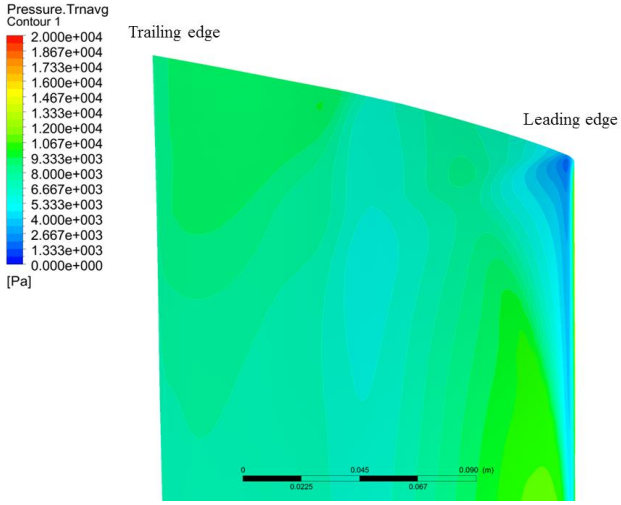


**Figure 24 Average static pressure at tip region of blade suction side with no tip model calculated by CFX**

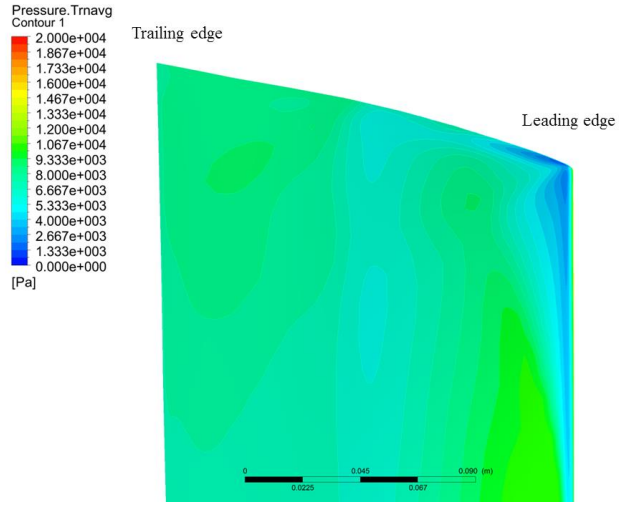


**Figure 25 Average static pressure at tip region of blade suction side with model with tip clearance calculated by CFX**

## 5 CONCLUSION

The effect of tip clearance flow on blade aerodynamic stability is analyzed in this study based on a realistic-scale last stage steam turbine model. A typical scale of tip clearance in steam turbines is applied in the model with tip clearance. Steady and unsteady simulation results on no tip clearance model solved by CFX and LUFT matches well with each other in steady state, and a phase difference is shown between solvers in the unsteady simulations.

The tip leakage flow generates a low Mach number region on the suction side of blade tip and influences the flow structure at the near tip region. In this model, the tip clearance flow has a stabilization effect on flutter at the first bending mode. The tip clearance flow does not have a significant effect on the overall shape of the damping curve. The stabilization effect happened at the suction side at near tip region. Two types of mechanisms contribute to the influence. The first type of mechanism is caused by the reduction of passage shock strength near the leading edge of the blade, and the second type is generated by the interaction between tip leakage flow and trailing edge wake from the neighbor blade. The two types of stabilization effect are both produced by the transonic flow field at the tip region.

Although considering tip clearance in the flutter boundary simulation would cost more computation resources, a significant difference of aerodynamic damping at the least stable IBPA could be found in this test case. Future work will be focused on the application of high-fidelity simulation method for a deeper understanding of this phenomenon.

## ACKNOWLEDGMENTS

The support provided by China Scholarship Council (CSC) during a visit of Tianrui Sun to KTH Royal Institute of Technology is acknowledged.

## REFERENCES

[1] Inoue M, Furukawa M. Physics of Tip Clearance Flow in Turbomachinery (Keynote Paper). ASME 2002 Joint US-European Fluids Engineering Division Conference. American Society of Mechanical Engineers, 2002: 777-789.

[2] Sjolander S A. Physics of tip-clearance flows. I & I I. Lecture series-van Kareman Institute for fluid dynamics, 1997, 1: B1-B34.

[3] Sanders A J, Hassan K K, Rabe D C. Experimental and numerical study of stall flutter in a transonic low-aspect ratio fan blisk. ASME Turbo Expo 2003, collocated with the 2003 International Joint Power Generation Conference. American Society of Mechanical Engineers, 2003: 339-348.

[4] Zhang M, Hou A, Zhou S, et al. Analysis on flutter characteristics of transonic compressor blade row by a fluid-structure coupled method. ASME Turbo Expo 2012: Turbine Technical Conference and Exposition. American Society of Mechanical Engineers, 2012: 1519-1528.

[5] Besem F M, Kielb R E. Influence of the Tip Clearance on a Compressor Blade Aerodynamic Damping. Journal of Propulsion and Power, 2016.

[6] Yang H, He L. Experimental study on linear compressor cascade with three-dimensional blade oscillation. Journal of propulsion and power, 2004, 20(1): 180-188.

[7] Fu Z, Wang Y, Jiang X, et al. Tip clearance effects on aero-elastic stability of axial compressor blades. Journal of Engineering for Gas Turbines and Power, 2015, 137(1): 012501.

[8] Teixeira M A M, Petrie-Repar P, Kameyama S. Tip Clearance Influence on Aeroelastic Stability of an Axial Turbine Blade Row. ISUAAAT 14; Stockhlom, Sweden, 8-11 September 2014. 2014.

[9] Glodic N, Vogt D, Fransson T. Influence of Tip Clearance Modelling in Predictions of Aeroelastic Response in an Oscillating LPT Cascade. ISUAAAT 13; Tokyo, Japan, 11-14 September 2012. 2012.

[10] Huang X, He L, Bell D L. Effects of Tip Clearance on Aerodynamic Damping in a Linear Turbine Cascade. Journal of Propulsion and Power, 2008, 24(1): 26-33.

[11] Riéra W, Marty J, Castillon L, et al. Zonal Detached-Eddy Simulation Applied to the Tip-Clearance Flow in an Axial Compressor. AIAA Journal, 2016: 2377-2391.

[12] Kelly R, Hickman A R, Shi K, et al. Very Large Eddy Simulation of a Transonic Axial Compressor Stage//52nd AIAA/SAE/ASEE Joint Propulsion Conference. 2016: 4745.

[13] Riéra W, Castillon L, Marty J, et al. Inlet condition effects on the tip clearance flow with zonal detached eddy simulation. Journal of Turbomachinery, 2014, 136(4): 041018.

[14] Petrie-Repar P, J, McGhee A, Jacobs P A, et al. Analytical maps of aerodynamic damping as a function of operating condition for a compressor profile. ASME Turbo Expo 2006: Power for Land, Sea, and Air. American Society of Mechanical Engineers, 2006: 1133-1144.

[15] Petrie-Repar P, J, McGhee A, Jacobs P A. Three-dimensional viscous flutter analysis of standard configuration 10. ASME Turbo Expo 2007: Power for Land, Sea, and Air. American Society of Mechanical Engineers, 2007: 665-674.

[16] Burton Z. Analysis of Low Pressure Steam Turbine Diffuser and Exhaust Hood Systems. Durham University, 2014

[17] Petrie-Repar P, Makhnov V, Shabrov N, et al. Advanced Flutter Analysis of a Long Shrouded Steam Turbine Blade. ASME Turbo Expo 2014: Turbine Technical Conference and Exposition. American Society of Mechanical Engineers, 2014: V07BT35A022-V07BT35A022.